DOI: https://doi.org/10.1016/j.talanta.2020.122029

Development of portable CdS QDs screen printed carbon electrode platform for electrochemiluminescence measurements and bioanalytical applications

*Beatriz Díez-Buitrago[1,2], Laura Saa[1], Nerea Briz[2], Valeri Pavlov[1]**

[1] Center for Cooperative Research in Biomaterials (CIC biomaGUNE), Basque Research and Technology Alliance (BRTA), Paseo de Miramon 182, 20014, Donostia San Sebastián, Spain

[2] Tecnalia, Basque Research and Technology Alliance (BRTA), Paseo Mikeletegi 2, 20009 Donostia-San Sebastián, Spain

* Valeri Pavlov: vpavlov@cicbiomagune.es

Abstract

In this work, a portable and disposable screen-printed electrode-based platform for CdS QDs electrochemiluminescence (ECL) detection is presented. CdS QDs were synthesized in aqueous media and placed on top of carbon electrodes by drop casting. The CdS QDs spherical assemblies consisted of nanoparticles about 4 nm diameters and served as ECL sensitizers to enzymatic assays. The nanoparticles were characterized by optical techniques, TEM and XPS. Besides, the electrode modification process was optimized and further studied by SEM and confocal microscopy. The ECL emission from CdS QDs was triggered with H_2O_2 as cofactor and enzymatic assays were employed to modulate the CdS QDs ECL signal by blocking the surface or generating H_2O_2 in situ. Thiol-bearing compounds such as thiocholine generated through the hydrolysis of acetylthiocholine by acetylcholinesterase interacted with the surface of CdS QDs thus blocking the ECL. The biosensor showed a linear range up to 5 mU mL^{-1} and a detection limit of 0.73 mU mL^{-1} for AChE. Moreover, the inhibition mechanism of the enzyme was studied by using 1,5-bis-(4-allyldimethylammonium-phenyl)pentan-3-one dibromide with a detection limit of 79.22 nM. Furthermore, the natural production of H_2O_2 from the oxidation of methanol by the action of alcohol oxidase was utilized to carry out the ECL process. This enzymatic assay presented a linear range up to 0.5 mg L^{-1} and a detection limit of 61.46 µg L^{-1} for methanol. The reported methodology shows potential applications for the development of sensitive and easy to hand biosensors and was applied to the determination of acetylcholinesterase and methanol in real samples.

Keywords: electrochemiluminescence; CdS QDs; biosensor; enzymatic modulation; portable instrumentation

Introduction

Electrochemiluminescence (ECL) is a powerful analytical tool that combines the simplicity of electrochemistry with its inherent sensitivity and a wide linear range chemiluminescence method [1]. ECL is the process whereby reactive species generated at electrodes undergo high-energy electron-transfer reactions to form excited states that emit light [2–6]. ECL is broadly applied in analytical chemistry, as well as in mechanism studies, as it provides not only the electrochemical information but also the spectrum data simultaneously, which gives very useful insight into the complex mechanisms [3]. This technique presents unique advantages such as high sensitivity, excellent temporal and spatial controllability, simplified optical setup, low background signal and no need of an external light source [4,5].

In the past few decades, many novel ECL emitters were synthesized and used in ECL reactions, for example luminol and ruthenium complex, etc. [4]. Nanomaterials with different sizes, shapes, chemical components and unique properties have been extensively adopted as an alternative for biosensing applications [7]. They offer several advantages such as the ability to enhance the efficiency of both biological element part and transducer part in many different ways within the biosensor platform [8,9]. Compared with conventional molecular emitters, nanomaterials have some distinctive merits such as size/surface-trap controlled luminescence and good stability against photobleaching. Most noteworthy, semiconductor nanocrystals also known as quantum dots (QDs) with unique optical and electrical properties have opened promising fields for new ECL emitters [10]. Since the first report on the ECL study of silicon nanoparticles [11], many elemental and compound semiconductor QDs have been developed to apply in ECL analytical techniques. Recent works indicated that water-soluble QDs were excellent luminescent reagents for ECL systems, avoiding using toxic organic solutions and complicated modifying electrode procedures [12,13]. Previous works have demonstrated that ECL emission of QDs occurs via surface electron-hole recombination and are highly dependent on their surface states which can be tuned with desired element ratios and dopants to enhance the efficiency of the process [7,14,15]. The need of new formulations and easy and friendly procedures to get more efficient nanomaterials for ECL applications aimed to develop outstanding nanomaterials and platforms suitable for biosensors set up.

In electrochemiluminescence biosensors the light is detected upon ECL reaction at the application of a specific potential [4,6]. Highly sensitive photon detection is required and achieved by high performance detectors and further development to more sensitive and smaller sensor systems. This detection system presents great advantages over other optical techniques such as fluorescence. The mechanism doesn't require an external light source so light scattering and the background signal are reduced, reaching higher signal-to-noise ratios and lower limits of detection. Besides, ECL is highly localized and time-triggered detection method, since the reaction only takes places at the potential application [16].

ECL devices display great potential for miniaturization because of its few hardware requirements. The power source can be supplied with a battery [17], the electrodes can be design at a microscale size[18] and the light sensors could be integrated via small photodiodes [19]. This combined with the advances in miniaturization systems could fulfil the current need of portable instruments for fast analytical determination in situ. Usually ECL devices are controlled by an external potentiostat or an amperometric unit that establishes potential differences or electric current to the electrodes. The photon detector utilized will depend on the practical requirements of the final system. When no size restriction is applied, a good solution is the use of a photomultiplier tube (PMT) which presents a high sensitivity towards low amounts of photons, but they need very high voltage supply (up to thousands of volts) for a proper performance [20,21]. Moreover, the large dimension of these detectors makes then inadequate for portable instruments. Another technique for light detection is the use of a CCD camera [22]. Despite their good sensitivity, the main disadvantage of these devices is its complexity in their use and the need of low temperature working conditions to reach a good detection limit. On the other hand, photodiodes present features that make them appropriate for the design of a portable, miniaturized and handheld devices. Photodiodes have a small size, lower power consumption, they present less complex opto-electronic systems and they are cost-effective [19,23].

In order to meet the needs for portability, sensitivity and friendly fabrication process of an ECL biosensor, we proposed a CdS QDs QDs screen-printed carbon electrode sensing platform combined with a Si-photodiode integrated in an ECL cell for bioanalytical applications. The ECL portable device integrated a potentiostat/galvanostat and a Si-photodiode (µSTAT ECL, DropSens). Screen-printed carbon electrodes enabled the used of reduced volumes making the system cost-effective and simpler than conventional three electrode cells. Moreover, the surface modification with CdS QDs synthesized in aqueous solutions was carried out by simple but reproducible and stable adsorption. The applicability of our new CdS QDs-SPCE ECL portable device was validated for the detection of acetylcholinesterase and methanol in real samples. On the one hand, a variety of

methods have been developed for acetylcholinesterase determination such as electrometry, pH-stat, tintometry, radiometry and colorimetry [24]. These techniques provide sensitive and specific assays, but they lack miniaturization and portability. On the other hand, there have been developed several methods for the determination of methanol in the last century. The standard techniques include gas chromatography, Raman spectroscopy, surface plasmon resonance and refractive index [25–28]. All these techniques are highly sensitive, and they are commonly used in routine laboratories. However, they usually need specific work conditions and they are not easy to use out of the established facilities.

For the best of our knowledge, it is the first time that this ECL portable device is applied to a different system than luminol/$[Ru(pby)^3]^{2+}$ ECL classical reactions. These luminophores are commonly used because of their high luminescent efficiency that makes possible the use of less sensitive and portable detectors [29,30]. In this work, facile synthesis of CdS QDs was carried out to fabricate CdS QDs-SPCE that served as ECL efficient platform with high sensitivity towards enzymatic activity of some analytes of interest.

Experimental section

Chemicals

Cadmium nitrate ($Cd(NO_3)_2$), sodium sulfide (Na_2S), hydrogen peroxide, methanol, ethanol, alcohol oxidase (AOx) from Hansenula sp., acetylcholinesterase (AChE) from Electrophorus electricus sp., glucose oxidase type VII from Aspergillus Niger (GOx), acetylthiocholine chloride (ATCh), 1,5-bis-(4-allyldimethylammonium-phenyl)pentan-3-one dibromide (BW284c51), human serum (HS) and other chemicals were purchased from Sigma-Aldrich. Anhydrous D (+)-glucose was purchased from PanReac AppliChem. The alcoholic beverage (vodka) was purchased in local supermarket in San Sebastián (Spain).

Apparatus

Fluorescence measurements were performed on a Varioskan Flash microplate reader (Thermo Scientific) using black microwell plates at room temperature. The system was controlled by the SkanIt Software 2.4.3. RE for Varioskan Flash. Electrochemical and electrochemiluminescence measurements were recorded with a potentiostat/galvanostat (±4 V DC potential range, ±40 mA maximum measurable current) and Si-photodiode integrated in the ECL cell, combined in one portable instrument (DropSens S.L., Spain). The ECL equipment was controlled by the specific software DropView 8400. Disposable screen-printed carbon electrodes (SPCEs; DRP-110;

DropSens) were employed as the electrode surface throughout this work. Transmission electron microscopy (TEM) images were recorded with a JEOL JEM 2100F microscope equipped with a high-angle annular dark field (HAADF) detector operating at 120 kV. Scanning electron microscopy (SEM) images were recorded with a JEOL JSM-6490LV at 15 kV, running in a point by point scanning mode with a dual beam FIB-FEI Helios 450S microscope. Confocal microscopy was carried out with a Zeiss Axio Observer epifluorescence microscope. Images were acquired with a 20x (air, NA 0.8) objective, in reflection mode, using excitation 365nm LED at 48% power and an emission filter for DAPI (ex 335/383 and em 420/470nm). AxiocamMR R3 detector was used for acquisition, exposure adjust to 2 s. Microscope controlled with Zen blue software v2.3 also used for image processing. X-ray photoelectron spectroscopy (XPS) experiments were performed in a SPCES Sage HR 100 spectrometer with a non-monochromatic X-ray source (Aluminum Kα line of 1486.6 eV energy and 253 W) placed perpendicular to the analyzer axis and calibrated using the 3d5/2 line of Ag with a full width at half maximum (FWHM) of 1.1 eV.

Methods

CdS QDs synthesis and CdS QDs-SPCE fabrication

Varying amounts of $Cd(NO_3)_2$ and Na_2S were mixed up in tris-HCl 5 mM pH=8 for 5 min at room temperature. After that, the fluorescence spectra of the resulting CdS QDs were recorded at λexc=280 nm. For the fabrication of the biosensor the SPCEs were pretreated electrochemically by cyclic voltammetry (CV) at a potential range from 0 to 0.6 V in tris-HCl 5 mM pH=8 buffer at 50 mV s^{-1}. Subsequently, a 7 µL drop of CdS QDs was drop casted on the SPCEs and let dry at 37 °C during 1 h. Afterwards, CdS QDs-SPCEs were leave at room temperature overnight in dark. At last, SPCEs were washed with distilled water, dried under argon atmosphere and stored in the fridge.

Acetylcholinesterase enzymatic assay

Different amounts of AChE and ATCh were incubated in citrate-phosphate buffer pH=7.5 at 37 °C for 30 min. Next, a 40 µL drop was drop casted on the CdS QDs-SPCEs surface and let react at room temperature for 30 min. After that, CdS QDs-SPCEs were washed with buffer and dried under argon atmosphere. Finally, ECL measurements were recorded in a 60 µL drop of H_2O_2 10 mM in PBS with voltage scanned between 0 and -1.6 V at 50 mV s^{-1}.

Inhibition of acetylcholinesterase

Acetylcholinesterase (5 mU mL^{-1}) was incubated with different concentration of the inhibitor BW284c51 in citrate-phosphate buffer pH=7.5 at room temperature for 30 min. Next, a solution of

acetylthiocholine chloride (5 µL, 5 mM) was added to the mixture (45 µL) and incubated for 15 min at 37 °C. After that, 40 µL drop was drop casted on the CdS QDs-SPCEs surface and let react at room temperature for 30 min. Then, CdS QDs-SPCEs were washed with buffer and dried under argon atmosphere. Finally, ECL measurements were recorded in a 60 µL drop of H_2O_2 10 mM in PBS with voltage scanned between 0 and -1.6 V at 50 mV s^{-1}.

Alcohol oxidase enzymatic assay

Varying amounts of AOx and MeOH were incubated in citrate-phosphate buffer pH=7.5 at room temperature for 30 min. After that, ECL measurements were recorded in a 60 µL drop of the mixture with voltage scanned between 0 and -1.6 V at 50 mV s^{-1}. For ethanol interference studies, a mixture of methanol and ethanol was used following the same protocol.

Quantification of AChE and MeOH in real samples

Quantification of AChE in human serum and MeOH in vodka were performed by standard addition method. Samples of pooled human serum were centrifuged using Amicon Eltra filter with a 3000 molecular weight cutoff. After filtering, the serum was spiked with varying known concentrations of AChE. The respective ACHE concentration in these mixtures was then determined. The dilution factor of plasma in the assay was 1:600. Samples of vodka were spiked with known different concentrations of methanol. Thus, the corresponding final concentration of methanol in mixtures was determined as described above. The dilution factor of samples in the assay was 1:10000.

Results and discussion

Properties and characterization of synthesized CdS QDs

In this work, CdS QDs were synthesized by direct reaction of $Cd(NO_3)_2$ and Na_2S in tris-HCl buffer at room temperature with no capping agent. The resulting nanoparticles presented a light-yellow colour with a maximum absorbance peak at 460 nm and a broad fluorescence peak with a maximum at around 700 nm (Figure S1). From the spectral absorption edge, the diameter of CdS QDs could be calculated using Henglein's empirical curve that relates the wavelength of the absorption threshold (λem) to the diameter of the CdS QDs structures (2RCdS QDs=0.1 / (0.1338-0.0002345λem) nm) [31–34]. The mean diameters of the synthesized nanoparticles were calculated to be 3.86 nm. TEM and XPS data were further investigated to confirm the CdS QDs structures. TEM images from Figure 1 shows the CdS QDs with an average diameter of 3.89 nm, thus in agreement with the previous theoretical value. Even though there was no capping agent, sulphur and cadmium formed spherical nanoparticles aggregated in a big homogenous net as it has been

demonstrated in the literature [15,34–37]. Moreover, XPS analysis was performed to study the surface composition and the oxidation state of elements for solid state materials. As can be seen in Figure S2, almost all the cadmium and sulphur in the sample are forming Cd-S bonds. We also found some signals related to cadmium oxide and sulphur oxide on the surface as result of the easy metal oxidation in the air [35,38].

Properties and characterization of electrodes

For the biosensor platform, the CdS QDs synthesized were immobilized by simple adsorption on the surface of a screen-printed carbon electrode. The electrodes were first washed in buffer by cyclic voltammetry and dried under argon before their modification. Afterwards, a 7 µL drop of CdS QDs was placed on top of the working electrode and let dry at 37 °C for 1 h. Finally, they were kept overnight in dark at room temperature. The following day, the CdS QDs-SPCE were washed in buffer and dried under argon to ensure homogeneity and stored in the fridge for further utilization. SEM and confocal microscopy were carried out to characterize the resulting modified electrodes. SEM images evidenced the modification on the surface of the working electrode (Figure S3). In the images, the nanoparticles were homogeneously distributed all over the working electrode with no alteration of the rest electrodes even after the washing step. Carbon ink from the screen-printed electrodes is porous and presents a rough surface, enabling the adsorption of the nanoparticles with high stability. This approach is the simplest and most straight forward for the modification of the electrode surface and has been widely used in electrochemical biosensors [20,39–41]. In addition, confocal microscopy was performed to confirm the modification and stability of the modified electrodes. In Figure S4 the fluorescence spectroscopy images from three different electrodes are displayed: one bare electrode, one electrode with CdS QDs after 1 h of incubation at 37 °C, and the same electrode after washing step and stored for one day. The bare electrode didn't show any fluorescence because carbon ink is not fluorescence (Figure S4A). After the CdS QDs deposition, the fluorescence signal appeared from all the modified surface of the electrode (Figure S4B). Subsequently, the fluorescence slightly diminished due to the washing step and the removal of the CdS QDs excess on the surface (Figure S4C). The final electrode presented a homogeneous fluorescence signal coming from the CdS QDs adsorbed on the carbon surface even after their washing and storage in the fridge, thus confirming their stability.

Electrochemical and electrochemiluminescence behaviors of CdS QDs-SPCE

The ECL system presented is based on the light emission of the CdS QDs, as they are one of the most popular ECL emitters of semiconductor NCs [33,42–45]. This process was carried out in

presence of the oxidant H_2O_2, an important coreactant in cathodic ECL emission [14,15,36,42,46]. The proposed mechanism is described as follows. As the electrode potential was scanned to negative values, the CdS QDs were reduced to $(CdS)^{\bullet-}$ (eq 1) and the coreactant H_2O_2 was reduced to $OH^{\bullet}$ (eq 2). Then, $OH^{\bullet}$ could react with $(CdS)^{\bullet-}$ producing excited state (CdS)* (eq 3). Finally, when (CdS)* decayed back to the ground-state CdS, an intense emission was obtained (eq 4).

$$CdS + ne^- \rightarrow n(CdS)^{\bullet-} \quad (1)$$

$$H_2O_2 + e^- \rightarrow OH^- + OH^{\bullet} \quad (2)$$

$$(CdS)^{\bullet-} + OH^{\bullet} \rightarrow (CdS)^* + OH^- \quad (3)$$

$$(CdS)^* \rightarrow CdS + h\nu \quad (4)$$

Figure 2 shows the EC and ECL behaviors of our CdS QDs-SPCE in PBS containing 10 mM H_2O_2. Three cathodic peaks (P1, P2, P3) and one anodic peak (P4) were found at -0.46, -0.99, -1.29 and -1 V, respectively. Among them, P1 corresponded to the reduction of dissolved oxygen and P2 is assigned to the reduction of H_2O_2 as it can be seen for bare SPCE in presence of H_2O_2 [14,47]. P3 and P4 were attributed to the reduction and oxidation of CdS QDs [14,15,43,45] that only appeared in the CdS QDs-SPCE curves (Figure 2 and Figure S5A) and not for the control in bare SPCE (Figure S5B). Regarding the ECL curve, one peak was detected when scanning to negative potentials corresponding to CdS* emission (Figure 2 and Figure S5A), but not when analyzing the bare SPCE (Figure S5B) in presence of H_2O_2 10 mM. This peak is enhanced when adding H_2O_2 to CdS QDs-SPCE as we can see from the values of Figure 2 and Figure S5A.

Optimization of ECL working conditions

In order to achieve the optimal ECL response, the amount of cadmium for CdS QDs formation, the deposition volume and incubation temperature, the concentration of H_2O_2 and the reagent controls were carefully studied. In Figure S6 the ECL signals for cadmium calibration curve are presented. ECL signal increased with the concentration of cadmium added to a well-known sulphur solution (0.5 mM) reaching a plateau at 2 mM. The optimum volume for CdS QDs deposition was set at 7 µL, considering the working electrode size (4 mm) and the viscosity and surface tension of the CdS QDs solution. The incubation temperature for CdS QDs adsorption on the working electrode was compared in Figure S7. When incubating at 37 °C, the ECL signal obtained was more than three times higher than the one obtained when incubating at room temperature. Moreover, the concentration of the coreactant is one of the most important parameters for an optimum ECL signal. The ECL intensities from the calibration curve are shown in Figure S8. The ECL signal increased

when increasing H_2O_2 up to 10 mM. After that concentration, the ECL signal decrease because of the alteration of the surface due to the oxidant nature of the coreactant. Finally, we tested the ECL response of the SPCE modified with CdS QDs, $Cd(NO_3)_2$, Na_2S and with no modification in presence of H_2O_2 10 mM in PBS (Figure S9). Only CdS QDs-SPCE gave a high ECL signal and no significant peak was found for any of the controls. This result confirms the need of both reagents and a proper coreactant to yield an ECL signal.

The final values for the parameters studied were $Cd(NO_3)_2$ 2mM, H_2O_2 10 mM in PBS, 37 °C for CdS QDs adsorption and 7 µL CdS QDs volume. If nothing specified, this were the parameters used throughout the work.

ECL sensing application of CdS QDs-SPCE

The new CdS QDs-SPCE fabricated were employed as ECL sensing platform for biosensing. ECL biosensor can be fabricated based on several approaches, such as generation or depletion of coreactant catalyst [48,49], modulation of the communication between the electrode and coreactants by impedance effect [50] and promotion of electron transfer by compositing nanomaterials with ECL emitters [51]. With the previous studies, CdS QDs-SPCE were validated as sensitive ECL emitters by using H_2O_2 as cofactor regarding its good performance and suitability for ECL biosensors [52–55]. Taking this into account, we followed two different strategies for their application: affinity and direct assays.

Affinity assays were based on the interaction of the CdS QDs with the analyte of interest and the subsequent variation on the ECL intensities. Thiols were selected as model analyte regarding their strong interaction with CdS QDs surface [21,33,42,45,56–60]. In the proposed procedure, enzymatic assays were defined for the production of thiol-compounds capable of interact with the surface of our CdS QDs-SPCE. These thiols could link to the CdS QDs conferring hydrophobic properties to the surface and blocking the interaction with the H_2O_2. Considering this mechanism, we could associate the decrease in the ECL intensity with the enzymatic activity.

For the direct assays we took advantage of the natural enzymatic production of H_2O_2 of some bioassays to conduct the ECL process. This approach enables the direct use of enzymatic H_2O_2 as it can act as a ready-made coreactant for ECL emissions without the introduction of exogenous coreactants which makes the system neat, green, and facile [15,46,61,62].

Scheme 1 and 2 show the two applications of our modified electrodes. For the affinity assays, we used the enzymatic production of thiocholine from acetylthiocholine oxidation of acetylthiocholine

taking advantage of our expertise on previous works from the group [59,63,64]. The incubation of the enzyme with its substrate leads to the production of thiocholine in solution. Afterwards, CdS QDs-SPCE is kept in contact with the thiol solution and let react. After washing the electrodes, ECL measurements were carried out and the variation on the ECL intensity was related to the enzymatic activity (Scheme 1). For the direct assay, we selected the alcohol oxidase as model enzyme for H_2O_2 production [65–67]. Thus, in presence of methanol, this enzyme is able to produce enough amounts of the coreactant to yield the ECL process. In this case, the increase on the ECL intensities were correlated to the enzymatic activity (Scheme 2).

Affinity assays: acetylcholine enzymatic assay

The effect of varying concentrations of ATCh on the response of the present analytical system containing fixed amount of AChE (50 mU mL^{-1}) was studied. According to Figure 3A the response to increasing concentrations of ATCh is typical for an enzymatic system governed by the Michaelis-Menten kinetic model. One can notice the linear part of the calibration plot up to 0.05 mM of the substrate followed by the plot section approaching asymptotically the maximum response from 0.5 mM. The apparent Michaelis-Menten constant was calculated by fitting the experimental results to the equation $\Delta ECL = \Delta ECLmax[ATCh] / (KM + [ATCh])$. The value of 0.15 ± 0.034 mM correlated well with the literature data [59,68,69]. We calculated the LOD for ATCh (S/N=3) of 26.03 μM. This value was equal or even better than some amperometric procedures [70,71]. For subsequent experiments we selected a concentration of ATCh equal to 0.5 mM. Figure 3B shows the response of the analytical system to increasing amount of AChE at a fixed concentration of ATCh. The system demonstrated a linear decrease of the ECL signal from 0 to 5 mU mL^{-1} and reached a saturation point at around 50 mU mL^{-1}. The LOD for AChE was found at 0.73 mU mL^{-1} and it is lower than some amperometric [72], fiber-optic [73] and ECL [74] biosensors.

In order to provide more evidence that the biosensor platform is sensitive to AChE detection, we employed the cholinesterase inhibitor 1,5-bis-(4-allyldimethylammonium-phenyl)pentan-3-one dibromide (BW284c51), which has a mechanism of toxicity similar to organophosphorus nerve agents and is frequently utilized as an analogue of nerve gases [75–77]. This inhibitor has a high selectivity for AChE and competes with the enzyme substrate for binding to the active site in an reversible manner [77]. Figure 3C represents the ECL signal when pre-incubating the AChE with different amounts of BW. We observed that increasing amounts of BW were associated to an increase in the ECL signal related to the inhibition of the enzyme and the subsequent diminution in the amount of thiols produced. According to S/N = 3, we calculated a detection limit for BW of 79.22 nM similar to other fiber optic [78] and fluorogenic [63] methods.

Moreover, to validate the proposed system we used this method to determine AChE in commercially available HS. Different concentrations of the enzyme were added to diluted HS and the enzymatic activity was measured as previously described. We plotted the experimental data with the concentration of the standard (x-axis) against the ECL signal acquired (y-axis) (Figure 5A). A linear regression analysis was performed to calculate the intercept of the calibration curve with the x-axis, representing the concentration of AChE in the HS. Taking into consideration the dilution of the samples, the concentration of AChE was stablished at 5176 mU mL^{-1}. This value is similar to that reported in the literature for human plasma (5675±195 mU mL^{-1}) [59,79].

In addition, we also performed control experiments with different thiols to probe the mechanism of the presented system. We tested two pair of oxidized and reduced thiol compounds of interest in biosensing: cystine/cysteine (CSSC/CSH) and glutathione/oxidized glutathione (GSH/GSSG).

The interaction with the CdS QDs-SPCE surface was conducted by drop casting a 7 µL of the thiol solution on the working electrode for 20 min. After the washing step we measured their ECL behaviours in PBS with H_2O_2 10 mM. Only the reduced forms of the thiols (CSH and GSH) were able to interact with the CdS QDs on the outer layer and block the surface against the coreactant, thus decreasing the ECL signal (Figure S10). On the other hand, the oxidized form (CSSC and GSSG) didn't affect the ECL intensity of the CdS QDs-SPCE. These experiments confirmed our previous hypothesis regarding the selective interaction of our CdS QDs-SPCE surface towards thiol groups and its blocking for the interaction with the coreactant, decreasing the ECL signal.

Alcohol oxidase enzymatic assay

The influence on the ECL intensity of varying amounts of AOx in the presence of a fixed MeOH concentration (0.03 g L^{-1}) is shown in Figure 4A. The ECL intensity increased with increasing amounts of enzyme in the range studied. The determination of AOx using methanol as substrate demonstrated a LOD of 6.59 ng mL^{-1} (S/N=3). In Figure 4B is presented the calibration plot of varying amount of MeOH and a fixed concentration of AOx (0.05 µg mL^{-1}). The increased amounts of MeOH led to an increase in the ECL signal, as more H_2O_2 is produced in situ. The LOD for MeOH was calculated for 61.46 µg L^{-1} (1.92 µM). This ECL assay showed a better sensitivity than classical Raman spectroscopy [26] and amperometric biosensors [80,81].

Additionally, we applied this method to the detection of methanol in vodka. It is well known that methanol is toxic for humans and its content in alcoholic beverages must be controlled. Vodka was chosen as a model alcoholic beverage because of its high consumption, mostly in the Eastern European countries [82]. The same procedure of standard additions was performed. Known

quantities of methanol were added to vodka samples. By linear regression the amount of methanol was calculated as 13 mg L^{-1} (Figure 5B). This value was within the methanol levels permitted for alcohol beverages specified by the regulation (EC) No 110/2008, this value should not exceed 100 mg L^{-1}.

More evidence of the mechanism proposed was studied with a different enzymatic system. Glucose oxidase was selected because of its ability to produce H_2O_2 [83]. GOx is able to oxidize glucose in presence of oxygen yielding H_2O_2 that was used to carry out the ECL process. In Figure S11 is shown the ECL intensity results of two different GOx concentrations (3.5 and 1.5 mg mL^{-1}) in presence of glucose (2 mM) and the controls of individual reagents. ECL was only generated when the enzyme and substrate were present in solution and interacted to produce H_2O_2 that was used as ECL cofactor. Increasing amounts of enzyme produced a higher H_2O_2 concentration that led to an increase on the ECL intensity. No significant signal was detected when the reagents were analysed separately. With this additional prove of concept we could confirm our second hypothesis: the enzymatic production in situ of H_2O_2 can be used as ECL coreactant for our CdS QDs-SPCE, avoiding the use of an external reagent.

Conclusions

The need of portable, cheap and easy to hand devices for bioanalytical applications promotes the development of new strategies for its accomplishment. The present study shows a novel ECL platform based on CdS QDs with real bioanalytical applications on the detection of analytes of interest. The easy screen-printed electrode modification and the direct, facile and aqueous friendly synthesis of the nanoparticles simplifies the fabrication process of the final CdS QDs-SPCE ECL platform. Two approaches were carried out to modulate the ECL emission: enzymatic generation of thiols to block the CdS QDs surface and the in situ production of the H_2O_2 cofactor needed to produce the ECL signal. First, acetylcholinesterase was employed to release thiocholine that interacted with the CdS QDs thus decreasing the ECL signal. The inhibition mechanism of the enzyme was demonstrated by using the BW284c51. On the other hand, alcohol oxidase produced H_2O_2 and promoted the ECL signal when increasing the amounts of enzyme and substrate. Both strategies were applied to the detection of AChE and MeOH in real samples with successfully results. The proposed procedures are uncomplexed, cost effective and highly sensitive. To the best of our knowledge, this is the first time that this portable μ-STAT ECL device is employed for the direct detection of the CdS QDs ECL emission.

Acknowledgements

We thank Dr Desirè Di Silvio, surface analysis and fabrication platform, CIC biomaGUNE, for the XPS analysis.

Supporting Information

CdS QDs absorbance and fluorescence spectra, XPS analysis of CdS QDs, SEM images of CdS QDs-SPCE, fluorescence microscope images of CdS QDs-SPCE, cadmium calibration plot, temperature optimization, H2O2 calibration plot, ECL profile of CdS QDs-SPCE reagent controls, ECL signals of oxidized and reduced thiols, ECL signal of GOx/Glu system is available in the online version of this article at http://dx.doi.org/10.1007/**********).

Corresponding Author

* Valery Pavlov

CIC biomaGUNE, Basque Research and Technology Alliance (BRTA), Paseo Miramón 182, 20014 Donostia-San Sebastián, Spain

e-mail: vpavlov@cicbiomagune.es

Author contributions

The manuscript was written thought contributions of all authors. All authors have given approval to the final version of the manuscript.

Funding sources

This work was supported by the Ministry of Science, Innovation and Universities/AEI/FEDER, UE (RETOS I+D – Grant No.BIO2017-88030-R) and the Maria de Maeztu Units of Excellence Programme – Grant No. MDM-2017-0720) and Basque Government ELKARTEK program BMG17.

Notes

The authors declare no competing financial interest.

References

[1] B. Qiu, M. Miao, L. She, X. Jiang, Z.Y. Lin, G.N. Chen, An ultrasensitive biosensor for glucose based on solid-state electrochemiluminescence on GOx/CdS/GCE electrode, Anal. Methods. 5 (2013) 1941–1945. https://doi.org/10.1039/c3ay26419j.

[2] A.D.M. Wilkinson, A., IUPAC Compendium of Chemical Terminology, Blackwell Scientific Publications, Oxford, UK, 1997.

[3] A.J. Bard, Electrogenerated Chemiluminescence, CRC Press, 2004.

[4] M.M. Richter, Electrochemiluminescence (ECL), Chem. Rev. 104 (2004) 3003–3036. https://doi.org/10.1021/cr020373d.

[5] W. Miao, ChemInform Abstract: Electrogenerated Chemiluminescence and Its Biorelated Applications, ChemInform. 39 (2008) 2506–2553. https://doi.org/10.1002/chin.200841260.

[6] W. Miao, Electrogenerated chemiluminescence, Handb. Electrochem. (2007) 541–590. https://doi.org/10.1016/B978-044451958-0.50026-4.

[7] Y. Chen, S. Zhou, L. Li, J. jie Zhu, Nanomaterials-based sensitive electrochemiluminescence biosensing, Nano Today. 12 (2017) 98–115. https://doi.org/10.1016/j.nantod.2016.12.013.

[8] Z. Liu, W. Qi, G. Xu, Recent advances in electrochemiluminescence, Chem. Soc. Rev. 44 (2015) 3117–3142. https://doi.org/10.1039/c5cs00086f.

[9] J. Yao, L. Li, P. Li, M. Yang, Quantum dots: From fluorescence to chemiluminescence, bioluminescence, electrochemiluminescence, and electrochemistry, Nanoscale. 9 (2017) 13364–13383. https://doi.org/10.1039/c7nr05233b.

[10] J. Lei, H. Ju, Fundamentals and bioanalytical applications of functional quantum dots as electrogenerated emitters of chemiluminescence, TrAC - Trends Anal. Chem. 30 (2011) 1351–1359. https://doi.org/10.1016/j.trac.2011.04.010.

[11] Z. Ding, B.M. Quinn, S.K. Haram, L.E. Pell, B.A. Korgel, A.J. Bard, Electrochemistry and electrogenerated chemiluminescence from silicon nanocrystal quantum dots, Science (80-.). 296 (2002) 1293–1297. https://doi.org/10.1126/science.1069336.

[12] Q. Zhu, H. Liu, J. Zhang, K. Wu, A. Deng, J. Li, Ultrasensitive QDs based electrochemiluminescent immunosensor for detecting ractopamine using AuNPs and Au nanoparticles@PDDA-graphene as amplifier, Sensors Actuators, B Chem. 243 (2017) 121–

129. https://doi.org/10.1016/j.snb.2016.11.135.

[13] S.N. Ding, Y. Jin, X. Chen, N. Bao, Tunable electrochemiluminescence of CdSe@ZnSe quantum dots by adjusting ZnSe shell thickness, Electrochem. Commun. 55 (2015) 30–33. https://doi.org/10.1016/j.elecom.2015.03.011.

[14] Y.M. Fang, J. Song, R.J. Zheng, Y.M. Zeng, J.J. Sun, Electrogenerated chemiluminescence emissions from Cds nanoparticles for probing of surface oxidation, J. Phys. Chem. C. 115 (2011) 9117–9121. https://doi.org/10.1021/jp200521p.

[15] Y.Y. Zhang, H. Zhou, P. Wu, H.R. Zhang, J.J. Xu, H.Y. Chen, In situ activation of CdS electrochemiluminescence film and its application in H 2 S detection, Anal. Chem. 86 (2014) 8657–8664. https://doi.org/10.1021/ac501532y.

[16] S.E.K. Kirschbaum, A.J. Baeumner, A review of electrochemiluminescence (ECL) in and for microfluidic analytical devices, Anal. Bioanal. Chem. 407 (2015) 3911–3926. https://doi.org/10.1007/s00216-015-8557-x.

[17] W. Li, M. Li, S. Ge, M. Yan, J. Huang, J. Yu, Battery-triggered ultrasensitive electrochemiluminescence detection on microfluidic paper-based immunodevice based on dual-signal amplification strategy, Anal. Chim. Acta. 767 (2013) 66–74. https://doi.org/10.1016/j.aca.2012.12.053.

[18] N.P. Sardesai, K. Kadimisetty, R. Faria, J.F. Rusling, A microfluidic electrochemiluminescent device for detecting cancer biomarker proteins, Anal. Bioanal. Chem. 405 (2013) 3831–3838. https://doi.org/10.1007/s00216-012-6656-5.

[19] M.A. Carvajal, J. Ballesta-Claver, D.P. Morales, A.J. Palma, M.C. Valencia-Mirón, L.F. Capitán-Vallvey, Portable reconfigurable instrument for analytical determinations using disposable electrochemiluminescent screen-printed electrodes, Sensors Actuators, B Chem. 169 (2012) 46–53. https://doi.org/10.1016/j.snb.2012.01.072.

[20] J. Ballesta Claver, M.C. Valencia Mirón, L.F. Capitán-Vallvey, Disposable electrochemiluminescent biosensor for lactate determination in saliva, Analyst. 134 (2009) 1423–1432. https://doi.org/10.1039/b821922b.

[21] L. Lu, J. Wu, M. Li, T. Kang, S. Cheng, Detection of DNA damage by exploiting the distance dependence of the electrochemiluminescence energy transfer between quantum dots and gold nanoparticles, Microchim. Acta. 182 (2015) 233–239.

https://doi.org/10.1007/s00604-014-1322-6.

[22] K. Kadimisetty, S. Malla, N.P. Sardesai, A.A. Joshi, R.C. Faria, N.H. Lee, J.F. Rusling, Automated multiplexed ecl immunoarrays for cancer biomarker proteins, Anal. Chem. 87 (2015) 4472–4478. https://doi.org/10.1021/acs.analchem.5b00421.

[23] M.A. Carvajal, J. Ballesta-Claver, A. Martínez-Olmos, L.F. Capitán-Vallvey, A.J. Palma, Portable system for photodiode-based electrochemiluminescence measurement with improved limit of detection, Sensors Actuators, B Chem. 221 (2015) 956–961. https://doi.org/10.1016/j.snb.2015.07.038.

[24] V.E. V St Omer, G.E. Rottinghaus, Clinical and Experimental Toxicology of Organophosphates and Carbamates, in: B. Ballantyne, T.C.B.T.-C. and E.T. of O. and C. Marrs (Eds.), Butterworth-Heinemann, 1992: pp. 15–27. https://doi.org/https://doi.org/10.1016/B978-0-7506-0271-6.50008-5.

[25] M.-L.L. Wang, J.-T.T. Wang, Y.-M.M. Choong, A rapid and accurate method for determination of methanol in alcoholic beverage by direct injection capillary gas chromatography, J. Food Compos. Anal. 17 (2004) 187–196. https://doi.org/https://doi.org/10.1016/j.jfca.2003.08.006.

[26] I.H. Boyaci, H.E. Genis, B. Guven, U. Tamer, N. Alper, A novel method for quantification of ethanol and methanol in distilled alcoholic beverages using Raman spectroscopy, J. Raman Spectrosc. 43 (2012) 1171–1176. https://doi.org/10.1002/jrs.3159.

[27] M.G. Manera, G. Leo, M.L. Curri, P.D. Cozzoli, R. Rella, P. Siciliano, A. Agostiano, L. Vasanelli, Investigation on alcohol vapours/TiO2 nanocrystal thin films interaction by SPR technique for sensing application, Sensors Actuators B Chem. 100 (2004) 75–80. https://doi.org/https://doi.org/10.1016/j.snb.2003.12.025.

[28] Y. Tai, M. Pan, E. Lin, D. Huang, P. Wei, Quality Detection of Alcoholic Beverages Using Optical Fiber Tips, IEEE Sens. J. 16 (2016) 5626–5631. https://doi.org/10.1109/JSEN.2016.2571307.

[29] A. Habekost, Rapid and sensitive spectroelectrochemical and electrochemical detection of glyphosate and AMPA with screen-printed electrodes, Talanta. 162 (2017) 583–588. https://doi.org/10.1016/j.talanta.2016.10.074.

[30] M.M.P.S. Neves, P. Bobes-Limenes, A. Pérez-Junquera, M.B. González-García, D.

Hernández-Santos, P. Fanjul-Bolado, Miniaturized analytical instrumentation for electrochemiluminescence assays: a spectrometer and a photodiode-based device, Anal. Bioanal. Chem. 408 (2016) 7121–7127. https://doi.org/10.1007/s00216-016-9669-7.

[31] L. Spanhel, M. Haase, H. Weller, A. Henglein, Photochemistry of Colloidal Semiconductors. 20. Surface Modification and Stability of Strong Luminescing CdS Particles, J. Am. Chem. Soc. 109 (1987) 5649–5655. https://doi.org/10.1021/ja00253a015.

[32] S.S. Narayanan, S.K. Pal, Aggregated CdS quantum dots: Host of biomolecular ligands, J. Phys. Chem. B. 110 (2006) 24403–24409. https://doi.org/10.1021/jp064180w.

[33] J.X. Liu, S.N. Ding, Multicolor electrochemiluminescence of cadmium sulfide quantum dots to detect dopamine, J. Electroanal. Chem. 781 (2016) 395–400. https://doi.org/10.1016/j.jelechem.2016.08.027.

[34] Y.Y. Zhang, Q.M. Feng, J.J. Xu, H.Y. Chen, Silver Nanoclusters for High-Efficiency Quenching of CdS Nanocrystal Electrochemiluminescence and Sensitive Detection of microRNA, ACS Appl. Mater. Interfaces. 7 (2015) 26307–26314. https://doi.org/10.1021/acsami.5b09129.

[35] H. Huang, J. Li, J.J. Zhu, Electrochemiluminescence based on quantum dots and their analytical application, Anal. Methods. 3 (2011) 33–42. https://doi.org/10.1039/c0ay00608d.

[36] H. Zhou, T. Han, Q. Wei, S. Zhang, Efficient Enhancement of Electrochemiluminescence from Cadmium Sulfide Quantum Dots by Glucose Oxidase Mimicking Gold Nanoparticles for Highly Sensitive Assay of Methyltransferase Activity, Anal. Chem. 88 (2016) 2976–2983. https://doi.org/10.1021/acs.analchem.6b00450.

[37] S.P. Based, Highly Sensitive Electrochemiluminescence Detection of Single-Nucleotide Polymorphisms Based on Isothermal Cycle-Assisted Triple-Stem Probe with Dual-Nanoparticle Label, Anal. Chem. 83 (2011) 8320–8328. https://doi.org/10.1021/ac2022629.

[38] D.P. Griffis, R.W. Linton, Quantitative comparison of direct and derivative AES with XPS of metal sulfides, Surf. Interface Anal. 4 (1982) 197–203. https://doi.org/10.1002/sia.740040505.

[39] M.Á.G. Rico, M. Olivares-Marín, E.P. Gil, Modification of carbon screen-printed electrodes by adsorption of chemically synthesized Bi nanoparticles for the voltammetric stripping detection of Zn(II), Cd(II) and Pb(II), Talanta. 80 (2009) 631–635.

https://doi.org/10.1016/j.talanta.2009.07.039.

[40] B.W. Lu, W.C. Chen, A disposable glucose biosensor based on drop-coating of screen-printed carbon electrodes with magnetic nanoparticles, J. Magn. Magn. Mater. 304 (2006) 400–402. https://doi.org/10.1016/j.jmmm.2006.01.222.

[41] J. Wang, W.W. Zhao, C.Y. Tian, J.J. Xu, H.Y. Chen, Highly efficient quenching of electrochemiluminescence from CdS nanocrystal film based on biocatalytic deposition, Talanta. 89 (2012) 422–426. https://doi.org/10.1016/j.talanta.2011.12.055.

[42] S.N. Ding, J.J. Xu, H.Y. Chen, Enhanced solid-state electrochemiluminescence of CdS nanocrystals composited with carbon nanotubes in H2O2 solution, Chem. Commun. (2006) 3631–3633. https://doi.org/10.1039/b606073k.

[43] T. Ren, J.Z. Xu, Y.F. Tu, S. Xu, J.J. Zhu, Electrogenerated chemiluminescence of CdS spherical assemblies, Electrochem. Commun. 7 (2005) 5–9. https://doi.org/10.1016/j.elecom.2004.10.005.

[44] W.W. Zhao, J. Wang, Y.C. Zhu, J.J. Xu, H.Y. Chen, Quantum Dots: Electrochemiluminescent and Photoelectrochemical Bioanalysis, Anal. Chem. 87 (2015) 9520–9531. https://doi.org/10.1021/acs.analchem.5b00497.

[45] Y. Shan, J.J. Xu, H.Y. Chen, Distance-dependent quenching and enhancing of electrochemiluminescence from a CdS:Mn nanocrystal film by Au nanoparticles for highly sensitive detection of DNA, Chem. Commun. (2009) 905–907. https://doi.org/10.1039/b821049g.

[46] S. Deng, H. Ju, Electrogenerated chemiluminescence of nanomaterials for bioanalysis, Analyst. 138 (2013) 43–61. https://doi.org/10.1039/c2an36122a.

[47] X.F. Wang, Y. Zhou, J.J. Xu, H.Y. Chen, Signal-on electrochemiluminescence biosensors based on CdS-carbon nanotube nanocomposite for the sensitive detection of choline and acetylcholine, Adv. Funct. Mater. 19 (2009) 1444–1450. https://doi.org/10.1002/adfm.200801313.

[48] H. Zhou, Y.Y. Zhang, J. Liu, J.J. Xu, H.Y. Chen, Efficient quenching of electrochemiluminescence from K-doped graphene-CdS:Eu NCs by G-quadruplex-hemin and target recycling-assisted amplification for ultrasensitive DNA biosensing, Chem. Commun. 49 (2013) 2246–2248. https://doi.org/10.1039/c3cc38990a.

[49] H. Niu, R. Yuan, Y. Chai, L. Mao, H. Liu, Y. Cao, Highly amplified electrochemiluminescence of peroxydisulfate using bienzyme functionalized palladium nanoparticles as labels for ultrasensitive immunoassay, Biosens. Bioelectron. 39 (2013) 296–299. https://doi.org/10.1016/j.bios.2012.06.004.

[50] B. Dai, L. Wang, J. Shao, X. Huang, G. Yu, CdS-modified porous foam nickel for label-free highly efficient detection of cancer cells, RSC Adv. 6 (2016) 32874–32880. https://doi.org/10.1039/c6ra01067a.

[51] G. Valenti, E. Rampazzo, S. Bonacchi, T. Khajvand, R. Juris, M. Montalti, M. Marcaccio, F. Paolucci, L. Prodi, A versatile strategy for tuning the color of electrochemiluminescence using silica nanoparticles, Chem. Commun. 48 (2012) 4187–4189. https://doi.org/10.1039/c2cc30612c.

[52] C.A. Marquette, S. Ravaud, L.J. Blum, Luminol electrochemiluminescence-based biosensor for total cholesterol determination in natural samples, Anal. Lett. 33 (2000) 1779–1796. https://doi.org/10.1080/00032710008543158.

[53] S.A. Kitte, W. Gao, Y.T. Zholudov, L. Qi, A. Nsabimana, Z. Liu, G. Xu, Stainless Steel Electrode for Sensitive Luminol Electrochemiluminescent Detection of H 2 O 2 , Glucose, and Glucose Oxidase Activity, Anal. Chem. 89 (2017) 9864–9869. https://doi.org/10.1021/acs.analchem.7b01939.

[54] H. Dai, Y. Chi, X. Wu, Y. Wang, M. Wei, G. Chen, Biocompatible electrochemiluminescent biosensor for choline based on enzyme/titanate nanotubes/chitosan composite modified electrode, Biosens. Bioelectron. 25 (2010) 1414–1419. https://doi.org/10.1016/j.bios.2009.10.042.

[55] X. Liu, L. Cheng, J. Lei, H. Liu, H. Ju, Formation of surface traps on quantum dots by bidentate chelation and their application in low-potential electrochemiluminescent biosensing, Chem. - A Eur. J. 16 (2010) 10764–10770. https://doi.org/10.1002/chem.201001738.

[56] D. Haye, D. Meisel, O.I. Mididb, Size control and properties of thiol capped CdS particles * T +, Colloids and Surfaces. 55 (1991) 121–136. https://doi.org/10.1016/0166-6622(91)80087-5.

[57] H. Li, W.Y. Shih, W.H. Shih, Synthesis and characterization of aqueous carboxyl-capped

CdS quantum dots for bioapplications, Ind. Eng. Chem. Res. 46 (2007) 2013–2019. https://doi.org/10.1021/ie060963s.

[58] S.S. Liji Sobhana, M. Vimala Devi, T.P. Sastry, A.B. Mandal, CdS quantum dots for measurement of the size-dependent optical properties of thiol capping, J. Nanoparticle Res. 13 (2011) 1747–1757. https://doi.org/10.1007/s11051-010-9934-1.

[59] G. Garai-Ibabe, L. Saa, V. Pavlov, Thiocholine mediated stabilization of in situ produced CdS quantum dots: Application for the detection of acetylcholinesterase activity and inhibitors, Analyst. 139 (2014) 280–284. https://doi.org/10.1039/c3an01662e.

[60] G. Jie, B. Liu, H. Pan, J.J. Zhu, H.Y. Chen, CdS nanocrystal-based electrochemiluminescence biosensor for the detection of low-density lipoprotein by increasing sensitivity with gold nanoparticle amplification, Anal. Chem. 79 (2007) 5574–5581. https://doi.org/10.1021/ac062357c.

[61] H. Jiang, H. Ju, Enzyme-quantum dots architecture for highly sensitive electrochemiluminescence biosensing of oxidase substrates, Chem. Commun. (2007) 404–406. https://doi.org/10.1039/b616007g.

[62] A. De Poulpiquet, B.D. Buitrago, M.D. Milutinovic, S. Arbault, L. Bouffier, A. Kuhn, N. Sojic, Dual enzymatic detection by bulk electrogenerated chemiluminescence, (2016). https://doi.org/10.1021/acs.analchem.6b01434.

[63] L. Saa, A. Virel, J. Sanchez-Lopez, V. Pavlov, Analytical applications of enzymatic growth of quantum dots, Chem. - A Eur. J. 16 (2010) 6187–6192. https://doi.org/10.1002/chem.200903373.

[64] A. Virel, L. Saa, V. Pavlov, Modulated Growth of Nanoparticles. Application for Sensing Nerve Gases, Anal. Chem. 81 (2009) 268–272. https://doi.org/10.1021/ac801949x.

[65] P. Kaszycki, H. Koloczek, Formaldehyde and methanol biodegradation with the methylotrophic yeast Hansenula polymorpha in a model wastewater system, 154 (2000) 289–296. https://doi.org/10.1016/S0944-5013(00)80002-6.

[66] B. Bucur, Æ.G. Lucian, Analysis of methanol – ethanol mixtures from falsified beverages using a dual biosensors amperometric system based on alcohol dehydrogenase and alcohol oxidase, (2008) 1335–1342. https://doi.org/10.1007/s00217-007-0662-4.

[67] J. Barroso, B. Díez-Buitrago, L. Saa, M. Möller, N. Briz, V. Pavlov, Specific bioanalytical optical and photoelectrochemical assays for detection of methanol in alcoholic beverages, Biosens. Bioelectron. 101 (2018) 116–122. https://doi.org/10.1016/j.bios.2017.10.022.

[68] M. Pohanka, M. Hrabinova, K. Kuca, J.P. Simonato, Assessment of acetylcholinesterase activity using indoxylacetate and comparison with the standard Ellman's method, Int. J. Mol. Sci. 12 (2011) 2631–2640. https://doi.org/10.3390/ijms12042631.

[69] M. Barteri, A. Pala, S. Rotella, Structural and kinetic effects of mobile phone microwaves on acetylcholinesterase activity, Biophys. Chem. 113 (2005) 245–253. https://doi.org/10.1016/j.bpc.2004.09.010.

[70] M. Kesik, F. Ekiz Kanik, J. Turan, M. Kolb, S. Timur, M. Bahadir, L. Toppare, An acetylcholinesterase biosensor based on a conducting polymer using multiwalled carbon nanotubes for amperometric detection of organophosphorous pesticides, Sensors Actuators B Chem. 205 (2014) 39–49. https://doi.org/10.1016/J.SNB.2014.08.058.

[71] G.L. Turdean, I.C. Popescu, L. Oniciu, D.R. Thevenot, Sensitive Detection of Organophosphorus Pesticides Using a Needle Type Amperometric Acetylcholinesterase-based Bioelectrode. Thiocholine Electrochemistry and Immobilised Enzyme Inhibition, J. Enzyme Inhib. Med. Chem. 17 (2002) 107–115. https://doi.org/10.1080/14756360290026469.

[72] B. Bucur, D. Fournier, A. Danet, J.L. Marty, Biosensors based on highly sensitive acetylcholinesterases for enhanced carbamate insecticides detection, Anal. Chim. Acta. 562 (2006) 115–121. https://doi.org/10.1016/j.aca.2005.12.060.

[73] R.A. Doong, H.C. Tsai, Immobilization and characterization of sol-gel-encapsulated acetylcholinesterase fiber-optic biosensor, Anal. Chim. Acta. 434 (2001) 239–246. https://doi.org/10.1016/S0003-2670(01)00853-4.

[74] S. Deng, J. Lei, L. Cheng, Y. Zhang, H. Ju, Biosensors and Bioelectronics Amplified electrochemiluminescence of quantum dots by electrochemically reduced graphene oxide for nanobiosensing of acetylcholine, Biosens. Bioelectron. 26 (2011) 4552–4558. https://doi.org/10.1016/j.bios.2011.05.023.

[75] A. Vale, S. Bradberry, P. Rice, T.C. Marrs, Chemical Warfare and Terrorism, Medicine (Baltimore). 31 (2004) 26–29. https://doi.org/10.1383/medc.31.9.26.27712.

[76] B.E. Mileson, J.E. Chambers, W.L. Chen, W. Dettbarn, M. Ehrich, A.T. Eldefrawi, D.W. Gaylor, K. Hamernik, E. Hodgson, A.G. Karczmar, S. Padilla, C.N. Pope, R.J. Richardson, D.R. Saunders, L.P. Sheets, L.G. Sultatos, K.B. Wallace, Common mechanism of toxicity: A case study of organophosphorus pesticides, Toxicol. Sci. 41 (1998) 8–20. https://doi.org/10.1006/toxs.1997.2431.

[77] L. Austin, W.K. Berry, Two selective inhibitors of cholinesterase, Biochem. J. 54 (1953) 695–700. https://doi.org/10.1042/bj0540695.

[78] W. Trettnak, F. Reininger, E. Zinterl, O.S. Wolfbeis, Fiber-optic remote detection of pesticides and related inhibitors of the enzyme acetylcholine esterase, Sensors Actuators B. Chem. 11 (1993) 87–93. https://doi.org/10.1016/0925-4005(93)85242-3.

[79] F. Worek, U. Mast, D. Kiderlen, C. Diepold, P. Eyer, Improved determination of acetylcholinesterase activity in human whole blood, Clin. Chim. Acta. 288 (1999) 73–90. https://doi.org/https://doi.org/10.1016/S0009-8981(99)00144-8.

[80] I. Kučera, V. Sedláček, An Enzymatic Method for Methanol Quantification in Methanol/Ethanol Mixtures with a Microtiter Plate Fluorometer, Food Anal. Methods. 10 (2017) 1301–1307. https://doi.org/10.1007/s12161-016-0692-2.

[81] D.-S. Park, M.-S. Won, R.N. Goyal, Y.-B. Shim, The electrochemical sensor for methanol detection using silicon epoxy coated platinum nanoparticles, Sensors Actuators B Chem. 174 (2012) 45–50. https://doi.org/10.1016/J.SNB.2012.08.017.

[82] P. Wiśniewska, M. Śliwińska, T. Dymerski, W. Wardencki, J. Namieśnik, The Analysis of Vodka: A Review Paper, Food Anal. Methods. 8 (2015) 2000–2010. https://doi.org/10.1007/s12161-015-0089-7.

[83] R. Wilson, A.P.D. Turner, Glucose oxidase: an ideal enzyme, Biosens. Bioelectron. 13 (1992) 165–185. https://doi.org/10.1016/0956-5663(92)87013-F.

Figures and figures caption

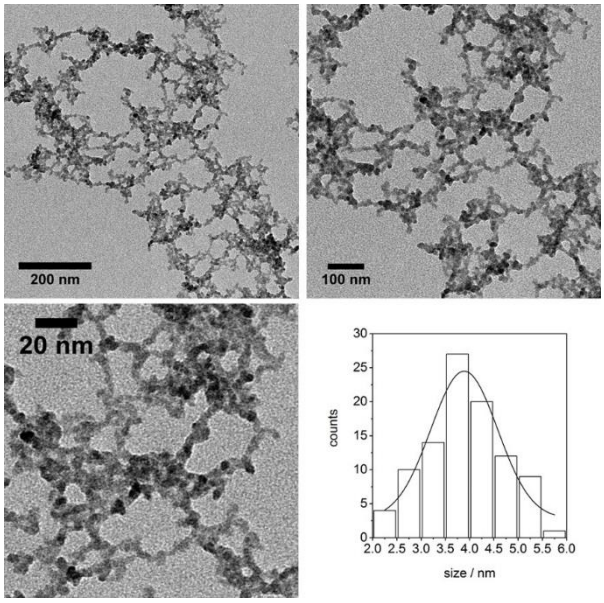

Figure 1. TEM images from CdS QDs and size histogram.

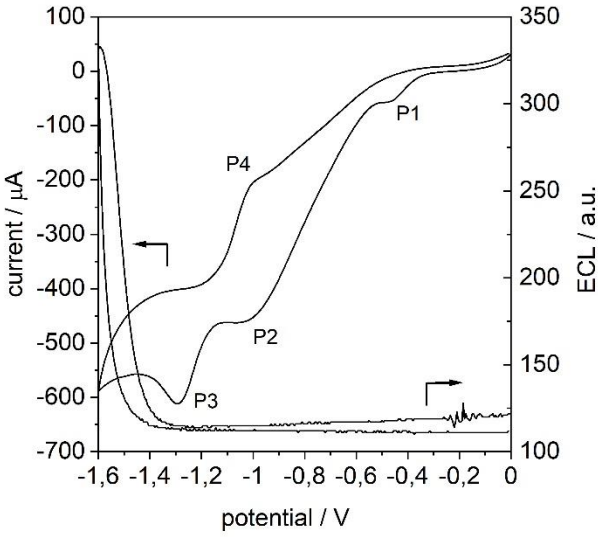

Figure 2. Cyclic voltammetry and ECL signals from CdS QDs-SPCE in presence of H_2O_2 50 mM in PBS.

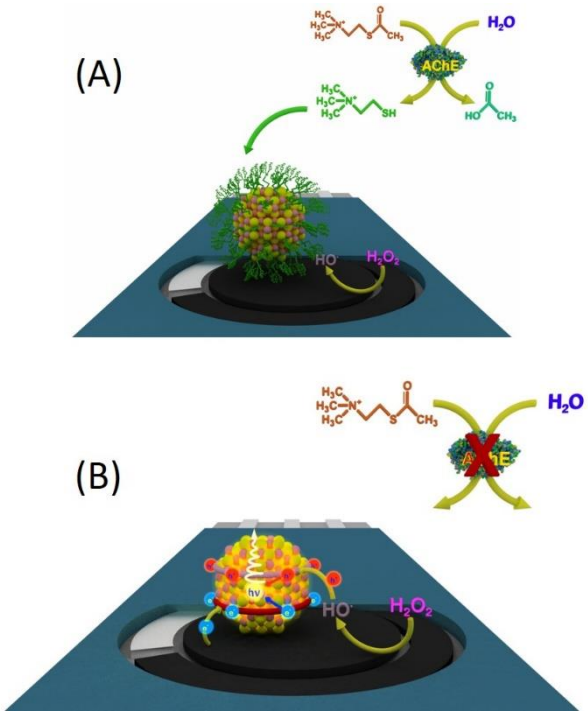

Scheme 1. (A) Enzymatic generation of thiocholine and interaction with the CdS QDs modified electrode. Blocking of the surface and diminution of the ECL signal. (B) Inhibition of AChE through BW inhibitor and increase of the ECL signal.

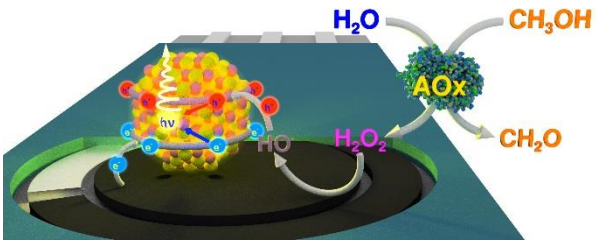

Scheme 2. Enzymatic generation of H_2O_2 and ECL performance.

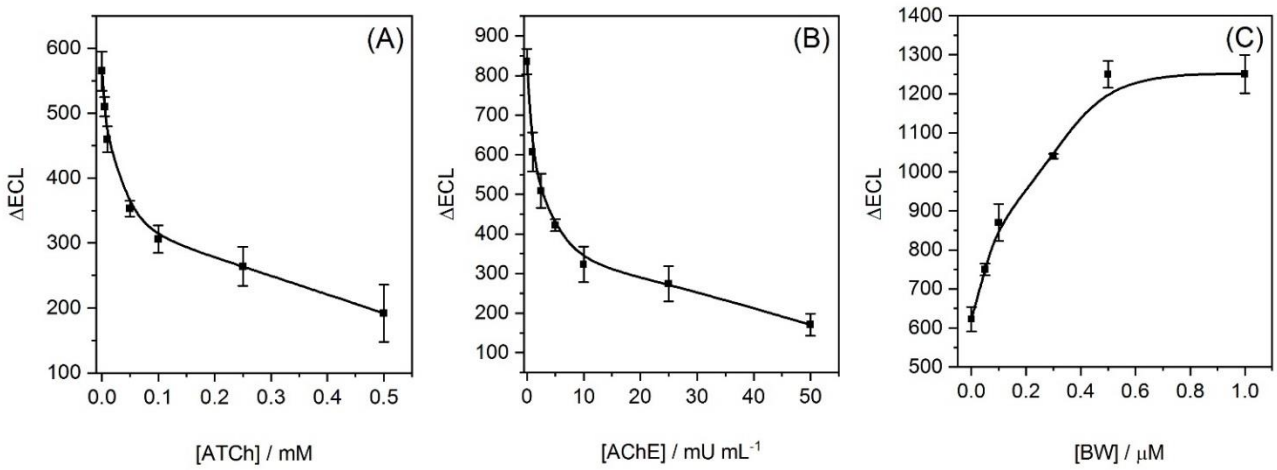

Figure 3. Calibration curves of (A) ATCh from 0 to 0.5 mM in presence of AChE 50 mU mL^{-1}, (B) AChE from 0 to 50 mU mL^{-1} in presence of ATCh 0.5 mM and (C) BW from 0 to 1 μM in presence of AChE 5 mU mL^{-1} and ATCh 0.5 mM, measured in PBS with H_2O_2 10 mM.

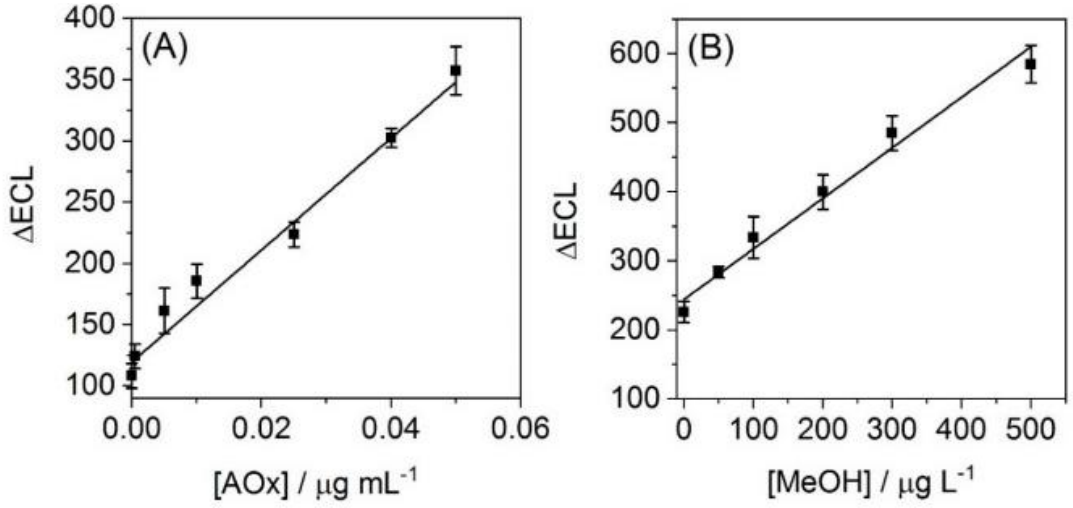

Figure 4. Calibration curves of (A) AOx from 0 to 0.05 μg mL^{-1} in presence of MeOH 0.03 g L^{-1}, (B) MeOH from 0 to 500 μg mL^{-1} in presence of AOx 0.05 μg mL^{-1}, measured in PBS with H_2O_2 10 mM.

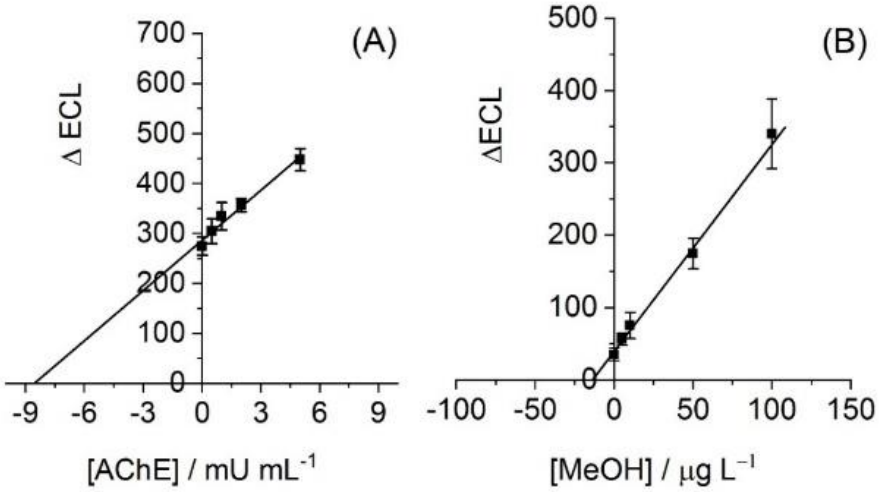

Figure 5. Quantification of (A) AChE in solutions containing different concentrations of added standard solution of AChE (from 0 to 5 mU mL^{-1}), ATCh (0.5 mM) and diluted HS; (B) MeOH in solutions containing different concentrations of added standard (from 0 to 100 μg L^{-1}), AOx (0.05 μg mL^{-1}) and diluted vodka.